Journal of Sound and Vibration (2000) **233**(2), 353–358
doi:10.1006/jsvi.1999.2807, available online at http://www.idealibrary.com on IDEAL®

LETTERS TO THE EDITOR

ON THE ACCURACY OF NEARFIELD PRESSURE PREDICTED BY THE ACOUSTIC BOUNDARY ELEMENT METHOD

S.-C. KANG AND J.-G. IH

Center for Noise and Vibration Control, Department of Mechanical Engineering, Korea Advanced Institute of Science and Technology, Science Town, Taejon 305-701, *Korea*

(*Received* 11 *August* 1999, *and in final form* 12 *November* 1999)

1. INTRODUCTION

The conventional boundary element method (CBEM) based on the Kirchhoff–Helmholtz boundary integral equation (BIE) is considered a very useful tool in calculating acoustical properties on a source surface or in a domain. Although this technique has many advantageous features in dealing with various acoustical problems, it inevitably suffers from the singularity problem in the close nearfield of a source surface. This problem is due to the singular kernel in the fundamental solution of BIE. In the three-dimensional acoustic problem, the fundamental solution corresponding to the monopole or dipole source is proportional to $1/R$ or $1/R^2$, where R means the distance between a surface point and a field point. When a field point is placed in the very close nearfield to the source surface, R becomes very small and thus an instability problem will arise in the numerical integration. This problem can be solved by adopting the non-singular boundary element method (NBEM) [1]. In this method, all singularities involved in the conventional BIE can be eliminated by subtracting two propagating plane wave components from the integral identity. With this method, a precise prediction of acoustical behavior is possible even in the very close nearfield to a source surface. Currently, precise nearfield prediction by BEM is considered important in various source identification techniques such as sound intensity scanning, energy streamline tracking [2], and nearfield acoustical holography [3].

In the close nearfield, where the distance z from the source surface is shorter than about 20% of the characteristic length, the field pressure predicted by CBEM has large errors (see figures in reference [1]). Although the reason for nearfield inaccuracy has been simply ascribed to the short distance between field points and the source surface, further detailed explanation in needed for this phenomenon. In this paper, acoustical characteristics of the predicted field are shown and the cause of this problem is explained in some detail. A pulsating sphere and a parallelepiped cavity are employed for illustrating the nearfield accuracy of field properties and the guidelines for precise prediction are given as a result. All formulations for CBEM and NBEM calculation are based on those in reference [1].

2. ANALYSIS AND DISCUSSION

The sound radiation from a uniformly pulsating sphere into the infinite homogeneous medium is chosen as an example for the exterior problem. When a sphere with a radius of

0022-460X/00/220353 + 06 $35.00/0

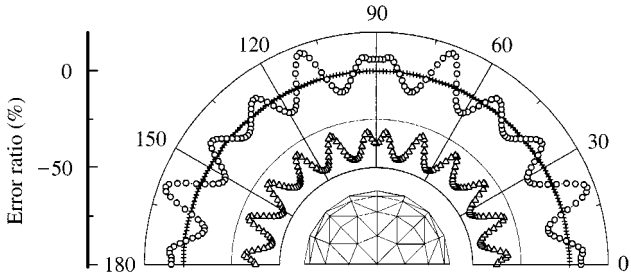

Figure 1. Directional pattern of predicted error ratio of field pressure for a pulsating sphere model at $ka = 1$ on the center plane ($N_G = 6$). Δ, CBEM and $(r - a)/L_C = 0{\cdot}01$; $\bigcirc$, CBEM and $(r - a)/L_C = 0{\cdot}1$; $+$, NBEM and $(r - a)/L_C = 0{\cdot}1$ or $0{\cdot}01$.

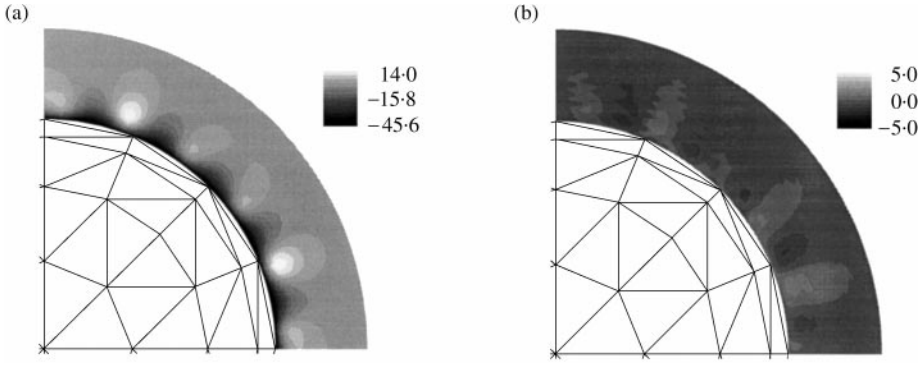

Figure 2. Predicted spatial distribution of error percentage of field pressure for a pulsating sphere model ($ka = 1$, $N_G = 6$). (a) CBEM, (b) NBEM.

a is pulsating with a harmonic surface velocity of $Ue^{j\omega t}$, the field pressure at a distance r from the origin is given by

$$p(r) = \frac{-\rho_0 cU}{r} \frac{jka^2}{(1 - jka)} \exp\{jk(r - a)\}, \tag{1}$$

where ρ_0, c, k denote the density, the speed of sound, and the wave number in the medium respectively. For BEM calculations, the boundary surface of pulsating sphere with a radius of 50 mm was discretized into 48 triangular, isoparametric and quadratic elements with 98 nodes. The maximum characteristics length, L_C, of the model was 52·1 mm.

Figure 1 shows the directional pattern of predicted field pressure on the horizontal plane passing through the center of the sphere model. One can observe a large and complicated oscillating error pattern of the CBEM results, whereas the use of NBEM yields very small errors in all directions that are less than $\pm$ 1%. When the distance from the surface is very small, e.g., $R \equiv r - a = 0{\cdot}01L_C$, the pressures predicted by CBEM are oscillating and under-estimated greatly in all directions. When the distance is increased to $R = 0{\cdot}1L_C$, the predicted directional values are either under- or overestimated compared to the true

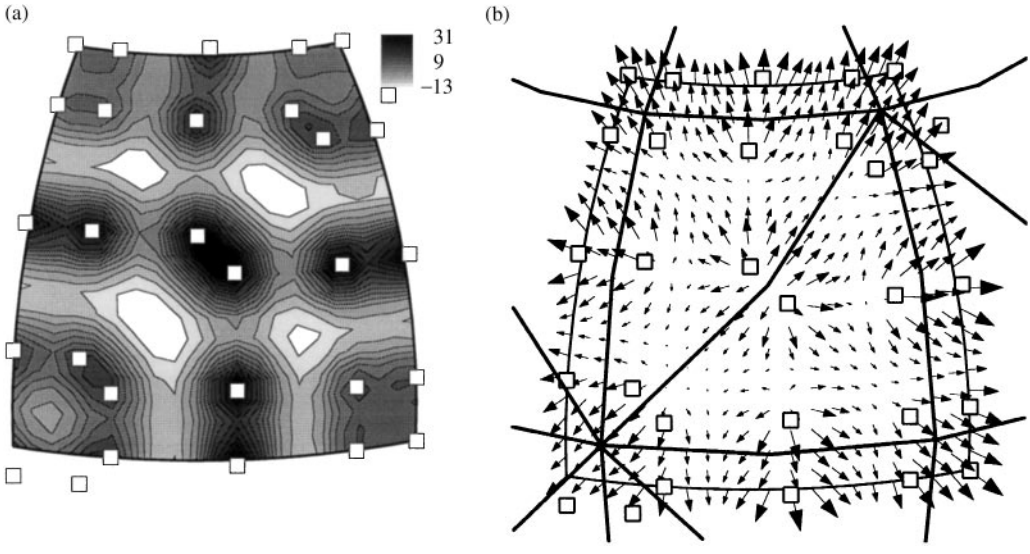

Figure 3. Predicted acoustic field properties by using CBEM for a pulsating sphere model at $ka = 1$ ($N_G = 6$, $R = 0{\cdot}1L_C$, square denotes the Gauss integration point). (a) Error percentage of field pressure amplitude, (b) active intensity vectors.

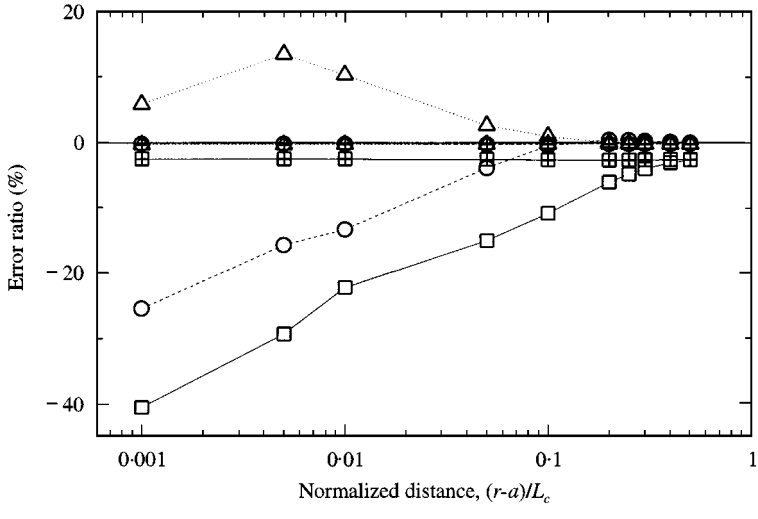

Figure 4. Mean error ratio of predicted field pressure of a pulsating sphere model at $ka = 1$. NBEM: —■—, $N_G = 1$; - - -⊕- - -, $N_G = 3$; ⋯△⋯, $N_G = 6$. CBEM: —□—, $N_G = 1$; - - -○- - -, $N_G = 3$; ⋯△⋯, $N_G = 6$.

pressure, but the pattern is nearly the same as in the former case. Figure 2 shows the calculated error ratio of field pressure on the horizontal plane. One can find that the error is large in the field very close to the Gauss integration points, and diminished to zero with an increase in distance.

In order to explain this phenomenon in detail, the error ratio is calculated at finely meshed field points covering more than two elements in tandem. In Figure 3, the error ratio of field pressure predicted by CBEM and the distribution of active intensity vectors are depicted when $R = 0{\cdot}1L_C$ and N_G is 6. Here, the discrete Gauss integration technique is

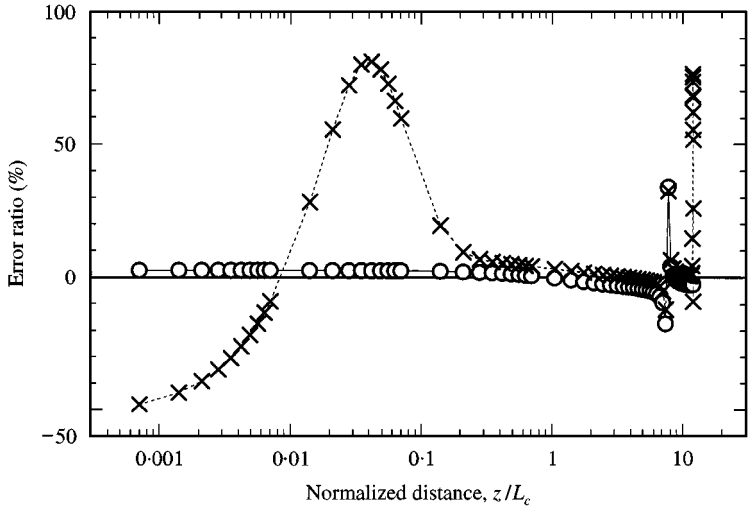

Figure 5. The error ratio of interior pressure by CBEM with increase of the longitudinal distance from the vibrating surface of a parallelepiped cavity: –○–, NBEM; - - × - -, CBEM.

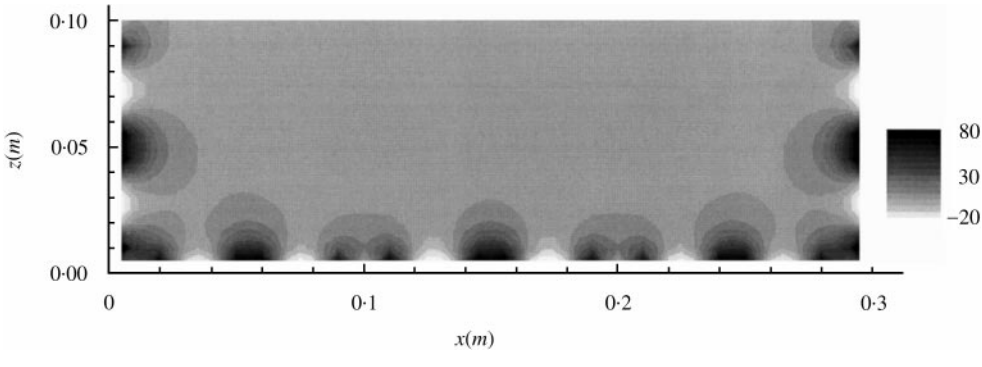

Figure 6. Spatial distribution of error percentage of predicted field pressure on the horizontal plane of the parallelepiped box interior due to a vibrating end face at 140 Hz.

employed in the numerical integration and N_G denotes the number of Gauss integration points. The area of the field plane is about 6·5% of the whole surface of the sphere and 1681 (i.e., 41×41 pattern) field points are distributed on this surface. Figure 3 explains graphically that the pressure on an element is subject to influence from the Gauss integration points in the adjacent elements. It is noted that the distribution of field pressure error is highly correlated with the distribution of Gauss integration points. Large errors can be formed especially at edges or corners of an element, where errors due to nearby integration points are superposed. From the plot of active intensity, one can find that the Gauss integration points behave like the acoustic sources. In the numerical integration within an element, the area integral of a function is approximated by the sum of weighted values of the function at pre-set points, namely, the Gauss integration points. Then, the positions of reference data change from the boundary nodes to the Gauss integration points in the numerical calculation process. Consequently, the singularity problem will occur at the Gauss integration points rather than the boundary nodes.

The predicted error ratio field pressure varying the radial distance is shown in Figure 4. In this calculation, the polar angle, the azimuth angle, the number of field points, and the area ratio to total spherical surface were the same as the foregoing computation and at each radial position. The mean level of error ratio is shown by changing the number of Gauss integration points. One can find that the mean error ratio by NBEM is nearly constant everywhere. The mean error ratio is about $-2{\cdot}5\%$ for $N_G = 1$, whereas it is less than $-0{\cdot}3\%$ for $N_G \geqslant 3$. The negative bias error is caused by the modelling error of BEM: a small difference in surface area and volume velocity of the BEM model from the ideal geometry. This error may be reduced by using the concept of effective radius [4]. CBEM yields large mean error in the close nearfield and the error decreases with increase in distance. In particular, when $N_G \geqslant 3$ and $R > 0{\cdot}2L_C$, the mean errors are less than $\pm 0{\cdot}5\%$. A data point at each radial distance in this figure corresponds to the mean value of 1681 points at each segmental field plane. It should be mentioned that the maximum error ratio at each field plane is very large and such an error occurs near the integration points. The maximum error ratio calculated by CBEM is about 200 times larger as compared to NBEM in the close nearfield of $R < 0{\cdot}2\ L_C$. This large error is generated by the singularity problem near the Gauss integration points. It is observed that the maximum error ratio cannot be reduced very much even if the number of integration points is increased.

A long parallelepiped with dimensions of $0{\cdot}3(w) \times 0{\cdot}3(h) \times 1{\cdot}7(l)\ \mathrm{m}^3$ was taken as an example of the interior problem. The boundary element model had 468 linear, triangular, isoparametric elements and 236 nodes. The maximum characteristic length of an element was 141·2 mm and N_G was 6. It was assumed that an end surface at $z = 0$ was vibrating as a rigid piston with a harmonic velocity of $(1 + \mathrm{j}1) \times 10^{-3}$ at 140 Hz and all other walls were rigid. The calculation frequency was chosen in order to avoid resonance and anti-resonance frequencies that would yield large numerical errors. Figure 5 shows the error ratio predicted by CBEM with an increase in the distance from the vibrating surface, and one can find large error at $z/L_C = 7{\cdot}8$ where a nodal plane exists. Figure 6 illustrates the spatial distribution of the predicted error by CBEM, where z denotes the longitudinal axis. The field pressure distribution is shown on a horizontal center plane in the interior field near the vibrating wall. Again, large errors can be observed near the Gauss integration points at every boundary and the error distribution pattern is nearly the same for all walls. It is also noted that the overall trend of CBEM and NBEM is similar to those shown in the foregoing figures for the exterior problem.

The reason why the calculation error is large near the Gauss integration points can be explained simply as follows. For a function f represented by a local co-ordinate (ξ, η), the discrete Gauss integration technique can be expressed as

$$\iint f(\xi, \eta)\, \mathrm{d}\xi\, \mathrm{d}\eta = \sum_{i=1}^{N_G} w_i f(\xi_i, \eta_i), \tag{2}$$

where w_i is the weighting factor for each integration point. Direct implementation of equation (2) in the BIE leads to a discretized BIE. Integral calculations diverge when the field point is located very close to the surface because the nature of singularities is not altered in the numerical process. In this calculation, the distance between surface points and field points are changed to those between Gauss points and field points. Consequently, the actual singularity problem will exist near Gauss integration points rather than surface points.

3. CONCLUSIONS

In this paper, the nearfield characteristics and accuracy of radiated acoustic field predicted by using BEM is investigated and discussed for two types of BIE formulations:

conventional and non-singular BIE. In the numerical process of BEM, the actual reference computation points are the Gauss integration points in the elements rather than the boundary nodes. Consequently, the singularity of fundamental solution in CBEM is generated near the Gauss integration points. The absolute mean error ratio is more than 5% when the distance from the surface is less than 5% of the characteristic length, when more than three integration points are used. However, it should be noted that the maximum local error ratio calculated by using CBEM is more than 100% in the close nearfield of $R < 0{\cdot}2L_C$, that is, about 200 times larger as compared to NBEM. It is found that large errors exist expecially at edges or corners due to the superposition of errors from nearby integration points including those in adjacent elements. The amount of mean nearfield error in using CBEM is highly affected by the number of Gauss integration points. However, the mean error ratio by NBEM is nearly constant everywhere and it is less than $-0{\cdot}3\%$ when more than three integration points are used. However, in using NBEM, one has to submit to an increase of calculation time and computer memory space in spite of the aforementioned advantages. When the BEM is used in energy streamlining or nearfield acoustical holography, one should carefully choose proper calculation techniques in order to predict the acoustic field properties in the nearfield precisely.

REFERENCES

1. B.-U. Koo, B.-C. Lee and J.-G. Ih 1996 *Journal of Sound and Vibration* **192**, 263–279. A non-singular boundary integral equation for acoustic problems.
2. R. V. Waterhouse and D. Feit 1986 *Journal of the Acoustical Society of America* **80**, 681–684. Equal-energy streamlines.
3. B.-K. Kim and J.-G. Ih 1996 *Journal of the Acoustical Society of America* **100**, 3003–3016. On the reconstruction of the vibro-acoustic field over the surface enclosing an interior space using the boundary element method.
4. D. C. Smith and R. J. Bernhard 1992 *Journal of Vibration and Acoustics, Transactions of the ASME* **114**, 127–132. Computation of acoustic shape design sensitivity using boundary element method.